Flex-grid optical networks : spectrum allocation and nonlinear dynamics of super-channels

Flex-grid optical networks: spectrum allocation and nonlinear dynamics of super-channels

Danish Rafique,[1,*] Talha Rahman,[1,2] Antonio Napoli,[1] Maxim Kuschnerov,[1] Gottfried Lehmann,[1] and Bernhard Spinnler[1]

[1]*Coriant R&D GmbH, St.-Martin-Str. 76, 81541, Munich, Germany*
[2]*Eindhoven University of Technology, Eindhoven, Netherlands*
[*]*danish.rafique@coriant.com*

Abstract: Flex-grid optical networks have evolved as a near-future deployment option to facilitate dynamic and bandwidth intense traffic demands. These networks enable capacity gains by operating on a flexible spectrum, allocating minimum required bandwidth, for a given channel configuration. It is thus important to understand the nonlinear dynamics of various high bit-rate super-channel configurations, and whether such channels should propagate homogenously (uniform channel configuration) or heterogeneously (non-uniform channel configuration), when upgrading the current static network structure to a flex-grid network. In this paper, we report on the spectrum allocation strategies based on the impact of inter-channel fiber nonlinearities, for PM-16QAM channels (240Gb/s, 480Gb/s and 1.2Tb/s) –termed as super-channels, propagating both homogenously, and heterogeneously with 120Gb/s PM-QPSK, 43Gb/s PM-QPSK, and 43Gb/s DPSK traffic. In particular, we show that for high dispersion fibers, both homogenous and heterogeneous spectrum allocation enable similar performance, i.e. the nonlinear impact of hybrid traffic is found to be minimal (less than 0.5dB relative penalties). We further report that in low dispersion fibers, the impact of spectrum allocation is more pronounced, and heterogeneous traffic employing 120Gb/s PM-QPSK neighbors enables the best performance, ~0.5dB better than homogenous transmission. However, the absolute nonlinear impact of co-propagating traffic is more significant, compared to high dispersion fibers, with maximum performance penalties up to 1.5dB.

OCIS codes: (060.1660) Coherent communications; (060.4250) Networks; (060.4254) Networks, combinatorial network design.

References and links

1. B. Mukherjee, "Issues and challenges in optical network design telecom network hierarchy," in *ECOC'11* (2011), Mo.1.K.
2. S. L. Woodward, "ROADM options in optical networks: flexible grid or not?," in *OFC'13* (2013), OTh3B.1.
3. M. Jinno, T. Ohara, Y. Sone, A. Hirano, O. Ishida, and M. Tomizawa, "Elastic and adaptive optical networks: Possible adoption scenarios and future standardization aspects," IEEE Commun. Mag. **49**(10), 164–172 (2011).
4. J. Elbers and A. Autenrieth, "From static to software-defined optical networks," Opt. Network Design Model. **12**, 1–4 (2012).
5. D. Rafique and A. D. Ellis, "Nonlinear penalties in long-haul optical networks employing dynamic transponders," Opt. Express **19**(10), 9044–9049 (2011).
6. C. Meusburger, D. A. Schupke, and A. Lord, "Optimizing the migration of channels with higher bitrates," J. Lightwave Technol. **28**(4), 608–615 (2010).
7. D. Rafique and A. D. Ellis, "Nonlinear penalties in dynamic optical networks employing autonomous transponders," IEEE Photonics Technol. Lett. **23**(17), 1213–1215 (2011).
8. Y. Huang, E. Ip, P. N. Ji, Y. Shao, T. Wang, Y. Aono, Y. Yano, and T. Tajima, "Terabit/s optical superchannel with flexible modulation format for dynamic distance/route transmission," in *OFC'12* (2012), OM3H.4.
9. N. Amaya, M. Irfan, G. Zervas, K. Banias, M. Garrich, I. Henning, D. Simeonidou, Y. R. Zhou, A. Lord, K. Smith, V. J. F. Rancano, S. Liu, P. Petropoulos, and D. J. Richardson, "Gridless optical networking field trial: flexible spectrum switching, defragmentation and transport of 10G/40G/100G/555G over 620-km field fiber," Opt. Express **19**(26), B277–B282 (2011).

#194912 - $15.00 USD Received 30 Jul 2013; revised 11 Oct 2013; accepted 15 Nov 2013; published 19 Dec 2013

10. L. Zong, G. N. Liu, A. Lord, Y. R. Zhou, and T. Ma, "40/100/400 Gb/s mixed line rate transmission performance in flexgrid optical networks," in *OFC'13* (2013), OTu2A.2.
11. M. Zhang, Y. Yin, R. Proietti, Z. Zhu, and S. J. B. Yoo, "Spectrum defragmentation algorithms for elastic optical networks using hitless spectrum retuning techniques," in *OFC'13* (2013), OW3A.4.
12. H. Y. Choi, T. Tsuritani, and I. Morita, "Feasibility demonstration of flexible Tx/Rx for spectrum defragmentation in elastic optical networks," in *OFC'13* (2013), OW3A.2.
13. J. G. Proakis and M. Salehi, *Digital Communications*, 5th ed. (McGraw-Hill, 2008), pp. 296–304.
14. C. Xia and D. van den Borne, "Impact of the channel count on the nonlinear tolerance in coherently-detected POLMUX-QPSK modulation," in *OFC'11* (2011), OWO1.
15. J. Renaudier, O. Bertran-Pardo, G. Charlet, M. Salsi, M. Bertolini, P. Tran, H. Mardoyan, and S. Bigo, "Investigation on WDM nonlinear impairments arising from the insertion of 100-Gb / s coherent PDM-QPSK over legacy optical networks," IEEE Photonics Technol. Lett. **21**(24), 1816–1818 (2009).
16. E. Tsardinakis, A. Lord, P. Wright, G. N. Liu, and P. Bayvel, "Should like demands be grouped in mixed line rate networks?," in *OFC'13* (2013), JW2A.65.
17. D. Rafique, S. Sygletos, and A. D. Ellis, "Intra-channel nonlinearity compensation for PM-16 QAM traffic co-propagating with 28 Gbaud m-ary QAM neighbours," Opt. Express **21**(4), 4174–4182 (2013).
18. S. Ma, B. Guo, Y. Zhao, X. Chen, J. Li, Z. Chen, and Y. He, "An investigation on power allocation between subcarriers with mixed formats in spectrum-flexible optical networks," in *ACP* (2012), AS4C.3.

1. Introduction

Recent growth in dynamic and bandwidth intense user-applications, cloud services, etc. has invoked high interest in flex-grid optical networks [1–3]. In order to cater for dynamic capacity demands, switchable transponders addressing the best possible combination of data-rate, spectral efficiency, spectral bandwidth, etc. can enable significant cost advantages to the network [4,5]. Although some form of elasticity can be ascertained from currently deployed fixed-grid networks, in terms of data-rate and spectral efficiency [6,7], it cannot be scaled indefinitely. For instance, in order to upgrade a 100Gb/s polarization multiplexed quadrature phase shifted keying (PM-QPSK) transponder with a 400G transponder option, the available choices could be a 100Gbaud PM-QPSK channel, or a 25Gbaud polarization multiplexed *m*-ary quadrature amplitude modulation (PM-256QAM) transponder, both of which are not practical at the moment. A 100Gbaud signal may not be generated due to limited components' bandwidth, on the other hand, PM-256QAM is not only difficult to realize, but is significantly distorted by both linear and nonlinear fiber impairments, essentially limiting the maximum transmission reach to ~100km [7].

On the other hand, in principle, full agility can be achieved from flex-networks. The concept of flex-networks allows for simultaneous transmission of mixed bit rates, 10Gb/s, 40Gb/s, 100Gb/s, 200Gb/s, 400Gb/s, 1Tb/s, etc., employing different modulation schemes and baud-rates, essentially allowing for flexible channel bandwidth, and spectral grid allocation dependent on the considered channel configuration [8,9]. However, one of the key unknowns in such flex-networks is the interplay of nonlinear fiber impairments when different mix of modulation formats, data-rate, and spectral grid are propagated together. Recently, a preliminary study was reported in [10], investigating the nonlinear impact of 40Gb/s and 100Gb/s channels on a 400Gb/s PM-16QAM super-channel, however a detailed analysis across various super-channel configurations, traffic allocations, and link configurations is still missing. Another important issue is the fragmentation scenario in flex-networks, due to spectrum allocation based on mixed traffic types, creating band-gaps across the spectrum, essentially reducing the capacity advantage [11,12].

In this paper, we extend the analysis of [10], and investigate the impact of fiber nonlinearities on various super-channel configurations, in the presence of different neighboring modulation formats at various data-rates, and consequently propose spectrum allocation strategies for such super-channels. We consider various high bit-rate channels employing PM-16QAM format, operating at 240Gb/s, 480Gb/s and 1.2Tb/s, with respective spectral widths of 37.5GHz, 75GHz, and 187.5GHz, respectively. The neighboring channels are either PM-16QAM super-channels (homogenous transmission), or 120Gb/s PM-QPSK, 43Gb/s PM-QPSK, and 43Gb/s differential phase shifted keying (DPSK) (heterogeneous transmission). We report that, on high dispersion fibers, the transmission performance, due to spectrum allocation of super-channels, is independent of the co-propagating traffic, and both

#194912 - $15.00 USD Received 30 Jul 2013; revised 11 Oct 2013; accepted 15 Nov 2013; published 19 Dec 2013

homogenous and heterogeneous spectrum allocation enable similar performance, with maximum absolute penalties of ~1dB. On the other hand, for low dispersion fibers, the impact of spectrum allocation is more significant, and co-propagating traffic employing 120Gb/s PM-QPSK enables the most optimum performance, however, homogenous traffic still performs within ~0.5dB of the optimal solution.

2. Transmission configurations

The simulation setup consisted of PM-16QAM central channel, at a fixed baud-rate of 30Gbaud, where different super-channel structures were modeled using 1-carrier (1C, 240Gb/s), 2-carriers (2C, 480Gb/s) and 5-carriers (5C, 1.2Tb/s). In order to minimize the impact of linear sub-carrier crosstalk, and dense spectral grid, spectral shaping was applied in digital domain, where the roll-off coefficient was fixed at 0.2. Moreover, the spacing within the subcarriers was also optimized, and fixed at ~1.15 × baud-rate. The super-channel structures for 1, 2 and 5 sub-carriers were set to have the spectral widths of 37.5GHz, 75GHz, and 187.5GHz, respectively. For all the sub-carriers both the polarization states were modulated independently using de-correlated bit sequences. Each digital sequence was de-multiplexed separately into two multi-level output symbol streams which were used to modulate an in-phase and a quadrature phase carrier. The optical transmitters consisted of continuous wave laser sources, followed by two nested Mach-Zehnder modulator structures for x- and y-polarization states. The two polarization states were combined using an ideal polarization beam combiner.

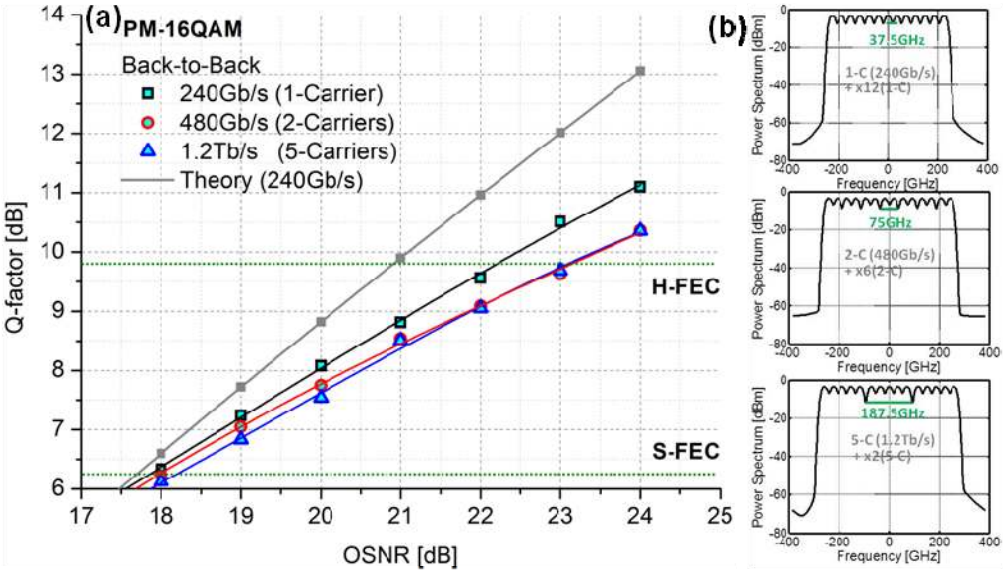

Fig. 1. a) Back-to-Back Q-factor as a function of OSNR, for various super-channel configurations, including, 240Gb/s 1-carrier (squares), 480Gb/s 2-carriers (circles), 1.2Tb/s 5-carriers (triangles), Theory 240Gb/s (grey line). b) Transmitter spectra for various super-channel configurations in Fig. 1(a), in a WDM format, where super-channel neighbor count is fixed at 12, 6, and 2 for 1C, 2C, and 5C PM-16QAM super-channels, respectively. H-FEC: Hard-decision FEC (error rate:1e-3), S-FEC: Soft-decision FEC (error rate:2e-2)

Figure 1(a) shows the back-to-back Q-factor (converted from BER) as a function of optical signal-to-noise ratio (OSNR) for the three super-channel configurations, along with the theoretical limit [13]. It can be seen that at Q-factor of 9.8 (BER of 1e-3), ~1.2dB OSNR penalty is observed for 1C scenario, compared to theory, which can be attributed to the realistic parameters used in the simulations. Moreover, when the number of carriers is increased to 2 and 5, 480Gb/s and 1.2Tb/s, respectively, the OSNR penalty increases to ~2.2dB. The additional penalties are observed since the subcarriers are densely packed with a

#194912 - $15.00 USD Received 30 Jul 2013; revised 11 Oct 2013; accepted 15 Nov 2013; published 19 Dec 2013

non-zero pulse roll-off factor. Note that we considered a practical roll-off factor, since fully Nyquist rectangular filters with 0 roll-off factor are unrealistic. On the other hand, at soft-decision forward error correction (FEC) threshold of 2e-2 (Q-factor of ~6.25dB), the OSNR penalty with respect to theory is reduced to <0.5dB, and the difference between any number of subcarriers is diminished due to noise dominance at such high error rate. In Fig. 1(b) we show the signal spectra at the transmitter for various super-channel configurations. Note that the super-channels are shown in a wavelength division multiplexing (WDM) format, where the number of neighbors for 1C, 2C, 5C PM-16QAM is fixed at 12, 6, and 2, respectively.

For WDM transmission two scenarios were considered, 1) Homogeneous transmission: Super-channels were transmitted in a WDM format, where for 1, 2 and 5 sub-carriers, 12, 6 and 2 neighboring super-channels were transmitted, respectively. 2) Heterogeneous transmission: The neighboring channels were considered to be 43Gb/s PM-QPSK (10.75Gbaud), 43Gb/s DPSK (43Gbaud), and 120Gb/s PM-QPSK (30Gbaud). The number of neighbors in this case was always fixed to 10 channels, and the spectral grid, within the heterogeneous neighboring traffic, was fixed at standard 50GHz, emulating a flex-grid network upgrade scenario.

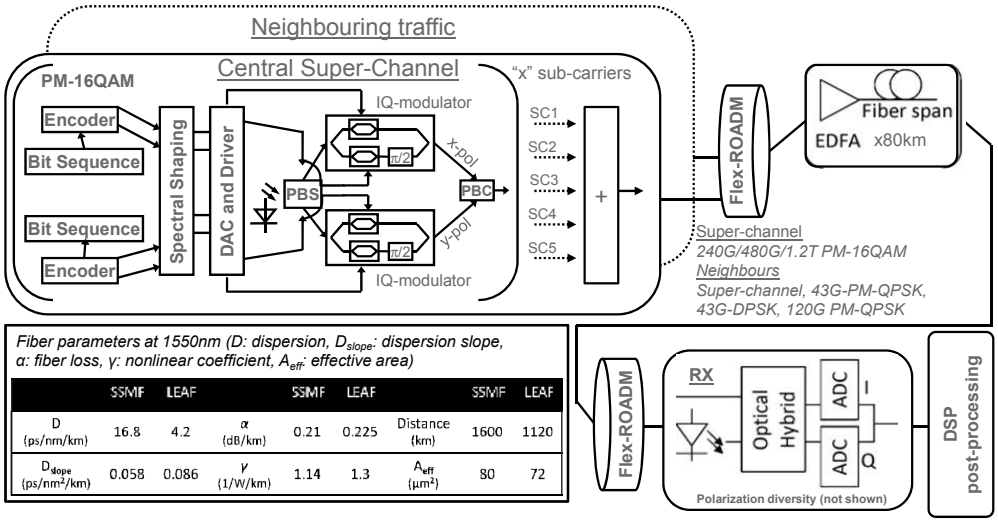

Fig. 2. Simulation setup for 30Gbaud PM-16QAM super-channels, employing 1(240Gb/s), 2(480Gb/s), and 5(1.2Tb/s) sub-carriers. The neighboring traffic is either super-channel themselves (homogeneous spectrum allocation), or 120Gb/s PM-QPSK, 43Gb/s DPSK, 43Gb/s PM-QPSK (heterogeneous spectrum allocation).

The signals were multiplexed, and propagated over two fiber types: standard single mode fiber (SSMF) and large effective area fiber (LEAF) (see inset of Fig. 2 for detailed parameters). As shown in Fig. 2, the transmission link consisted of 80 km spans, no inline dispersion compensation and single-stage erbium doped fiber amplifiers (EDFAs). Each amplifier stage was modeled with a 5 dB noise figure and the total amplification gain was set to be equal to the total loss in each span. At the coherent polarization diversity receiver, coherent channel selection was employed to de-multiplex the test sub-carrier (in case of 2- and 5-carrier transmission, first and third sub-carriers were evaluated). The signal was then detected using four balanced detectors to give the baseband electrical signal, sampled at ~2 samples per symbol. Transmission impairments were digitally compensated using conventional digital signal processing blocks, clock recovery, frequency domain dispersion compensation, polarization de-multiplexing, and carrier recovery. Finally, the symbol decisions were made, and the performance assessed by direct error counting (~400000bits, converted into Q-factor).

#194912 - $15.00 USD Received 30 Jul 2013; revised 11 Oct 2013; accepted 15 Nov 2013; published 19 Dec 2013

3. Results and discussions

3.1 Single super-channel transmission

Figure 3 shows Q-factor as a function of launch power per subcarrier for various super-channel configurations (240Gb/s, 480Gb/s, and 1.2Tb/s) for single super-channel transmission (representative of conventional single channel transmission). For the two fiber types, SSMF and LEAF, the maximum transmission distances were fixed at 1600km and 1120km, respectively, such that 1C transmission always achieves performance beyond soft FEC threshold (Q-factor of ~6.25). It can be seen that for any given configuration, at low power levels the performance is noise limited, and gradually reaches an optimum, beyond which it is degraded due to the impact of fiber nonlinearities. Furthermore, it is clear that for both fiber types, Figs. 3(a) and 3(b), 1C system enables the best performance, followed by 2C and 5C super-channels. This effect is simply due to sheer number of channels considered in the super-channel configuration, i.e. 1C essentially means single-channel transmission or only intra-channel nonlinearities, 2C and 5C also have the impact of inter-channel nonlinearities intrinsically included. However, it can also be seen that for LEAF, the performance penalty for 1C system is ~0.5dB, compared to SSMF. Moreover, for LEAF, the performance delta between 1C and 5C super-channels is around 1dB, compared to ~0.5dB in SSMF. This is attributed to channel-count dependency [14] and exacerbated nonlinearities in low dispersion fibers because of increased phase matching conditions.

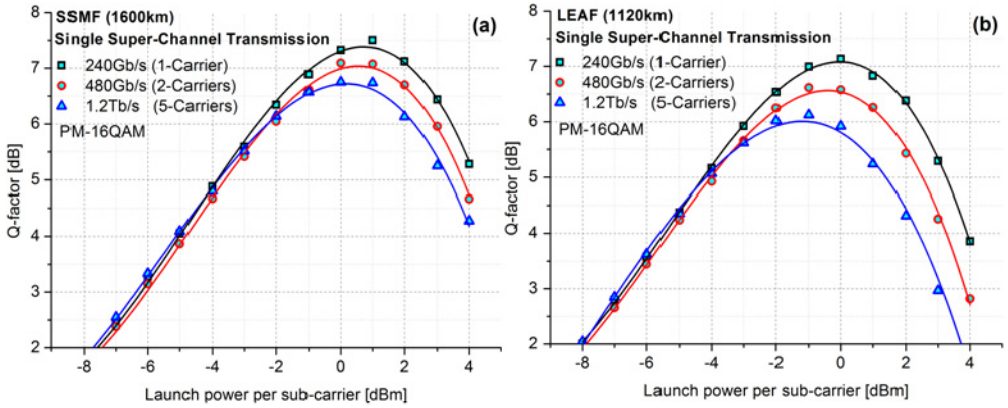

Fig. 3. PM-16QAM single super-channel transmission: Q-factor as a function of per subcarrier launch power. 240Gb/s 1-carrier (squares), 480Gb/s 2-carrier (circles), 1.2Tb/s 5-carrier (triangles), a) SSMF, 1600km, b) LEAF, 1120km.

3.2 WDM super-channel transmission

Having established the reference performance margins, in this section we investigate various spectrum allocation scenarios for super-channel transmission, employing either homogenous traffic (same format and configuration as the super-channel), and heterogeneous traffic (120Gb/s PM-QPSK, 43Gb/s PM-QPSK, 43Gb/s DPSK). Note that the launch power of neighboring traffic is fixed to near-optimal of 0dBm [7, 15], and launch power of the super-channel is varied. Figure 4(a) illustrates the transmission performance of 1C 240Gb/s, where single super-channel performance is plotted for reference. It can be seen that typically, the performance for both homogenous and heterogeneous transmission is similar, and achieves a maximum Q-factor of 7dB. However, in the presence of low baud-rate 43Gb/s PM-QPSK traffic, the performance is slightly degraded to 6.5dB due to exacerbated cross phase modulation effects. Likewise, for 2C 480Gb/s and 5C 1.2Tb/s, similar conclusions can be drawn, looking at Figs. 4(b) and 4(c). It can be seen that the net performance reduces, and the penalty delta between the homogenous and heterogeneous transmission even reduces further,

#194912 - $15.00 USD Received 30 Jul 2013; revised 11 Oct 2013; accepted 15 Nov 2013; published 19 Dec 2013

as number of sub-carriers are increased. This can be attributed to increased impact of densely packed subcarriers on the test sub-carrier, compared to the co-propagating traffic.

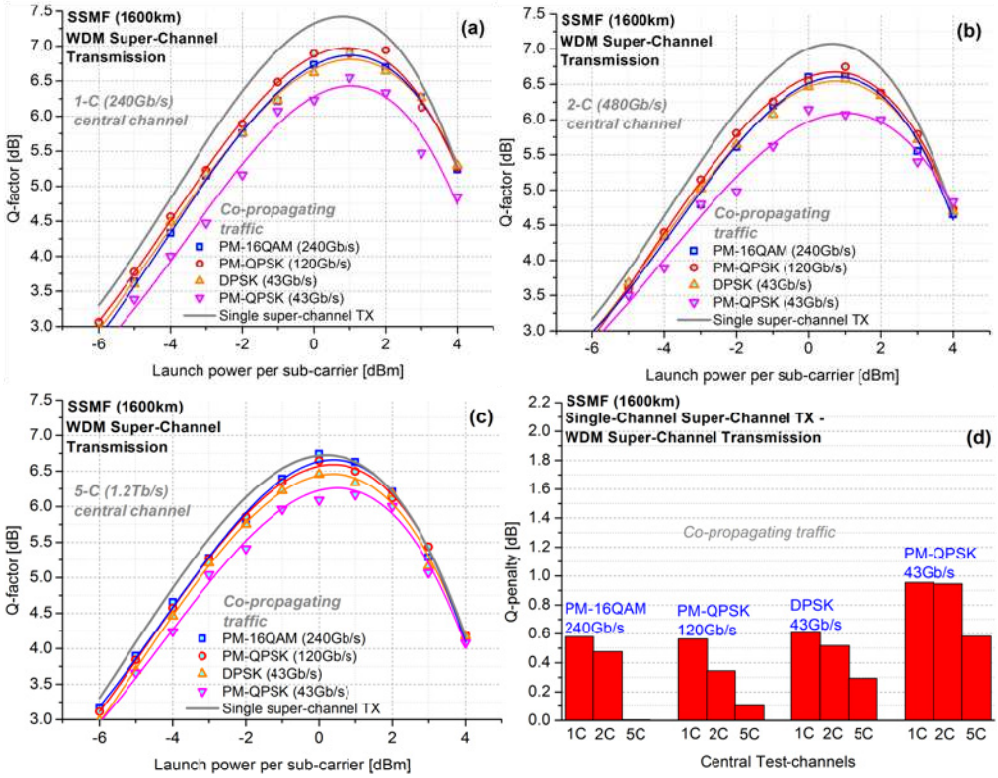

Fig. 4. PM-16QAM WDM super-channel transmission employing SSMF after 1600km. a) 240Gb/s 1-carrier, b) 480Gb/s 2-carriers, c) 1.2Tb/s 5-carriers. Homogeneous transmission employing super-channels themselves for Figs. 4(a)–4(c) (squares), Heterogeneous transmission: PM-QPSK 120Gb/s (circles), DPSK 43Gb/s (up-triangles), PM-QPSK 43Gb/s (down-triangles), Grey Lines (single super-channel transmission). d) Q-penalty for WDM super-channel transmission compared to single super-channel transmission, for all combinations in Figs. 4(a)–4(c).

In Fig. 4(d), we plot the Q-penalty for WDM transmission with respect to single-channel super-channel transmission; see Fig. 3(a). Two key attributes can be ascertained from this figure. Firstly, as the number of sub-carriers increases, the penalty reduces between single super-channel and WDM transmission, since progressively more channels are used in the super-channel itself, leading to greater cross channel nonlinearities within the super-channel. It is worth mentioning that although Q-penalty from the neighboring traffic reduces with increased number of sub-carrier, the absolute penalties increase with increasing sub-carrier count, as shown in Figs. 4(a)–4(c). Secondly, it can be seen that the Q-penalty is almost constant for homogeneous and heterogeneous transmission, and compared to single-super-channel transmission, the maximum performance degradation is only 0.5dB, i.e. in a network upgrade scenario, for non-dispersion managed system, the impact of inter-channel nonlinearities is very low. Although the penalty rises up to 1dB for 43Gb/s PM-QPSK, it is still within 0.5dB of the homogeneous transmission scenario,

This result indicates that in high dispersion fibers, the spectrum allocation may not play an important role from inter-channel fiber nonlinearities point of view, and homogeneous transmission may adequately be employed to suppress the fragmentation problem intrinsic to heterogeneous spectrum allocation. On the other hand, it also shows that depending on network type, i.e. static or fully dynamic, the spectrum allocation may be employed

#194912 - $15.00 USD Received 30 Jul 2013; revised 11 Oct 2013; accepted 15 Nov 2013; published 19 Dec 2013

independent of physical layer nonlinear impairments, and rather on metrics like network blocking probability, etc [16].

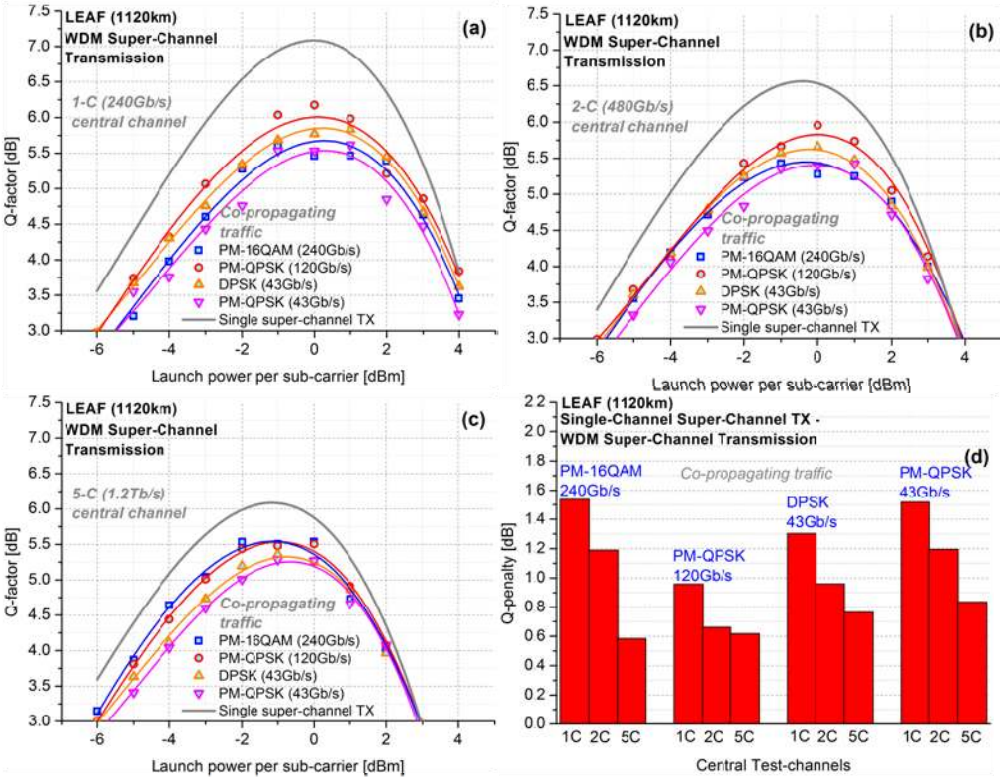

Fig. 5. PM-16QAM WDM super-channel transmission employing LEAF after 1120km. a) 240Gb/s 1-carrier, b) 480Gb/s 2-carriers, c) 1.2Tb/s 5-carriers. Homogeneous transmission employing super-channels themselves for Figs. 5(a)–5(c) (squares), Heterogeneous transmission: PM-QPSK 120Gb/s (circles), DPSK 43Gb/s (up-triangles), PM-QPSK 43Gb/s (down-triangles), Grey Lines (single super-channel transmission). d) Q-penalty for WDM super-channel transmission compared to single super-channel transmission, for all combinations in Figs. 5(a)–5(c).

In Fig. 5, we extend the spectrum allocation analysis for low dispersion fiber type, LEAF. It can be seen that, consistent with Fig. 4, the net performance decreases with increasing number of subcarriers. However, the difference in nonlinear performance for various traffic allocation strategies is more pronounced, compared to SSMF, due to increased impact of fiber nonlinearities owing to better phase matching conditions (reduced walk-off). In particular, it is clear that the heterogeneous traffic employing 120Gb/s PM-QPSK enables optimum performance for any given super-channel configuration. It can also be seen that for 1C and 2C systems, the optimum performance from PM-QPSK is followed by 43Gb/s DPSK, PM-16QAM (homogeneous transmission), and 43Gb/s PM-QPSK. Note that in this case PM-QPSK is the optimal solution because of increased nonlinear phase noise averaging owing to increased phase-states, compared to DPSK, higher baud-rate than 43Gb/s PM-QPSK, and phase-only modulation, compared to PM-16QAM. On the other hand, for 5-carrier super-channel configuration, the performance trend is similar to Fig. 4(c), owing to increased impact of inter-channel nonlinearities within the super-channel. Figure 5(d) plots the Q-penalty for WDM transmission, compared to single super-channel transmission. As discussed above, the 5C super-channel enables the least Q-penalty from neighboring traffic, although its absolute Q-factor is the lowest due to inter-channel crosstalk within the super-channel itself as shown in Fig. 5(c). More interestingly, the optimum performance is enabled by PM-QPSK

#194912 - $15.00 USD Received 30 Jul 2013; revised 11 Oct 2013; accepted 15 Nov 2013; published 19 Dec 2013

heterogeneous transmission, however, the homogenous traffic allocation is within 0.5dB of the optimum solution.

Nonetheless, our results confirm that in both high and low dispersion fiber types, homogeneous spectrum allocation may be employed, with limited penalties for low dispersion fibers (<~0.5dB) compared to the optimal solution of heterogeneous spectrum allocation. This additional penalty may be traded-off with the fragmentation problem in flex networks [16]. It is also worth mentioning that mutual power level optimization of various combinations of modulation formats may even further improve the performance [17,18].

4. Conclusion

We reported on spectrum allocation strategies for high and low dispersion fiber types, considering nonlinear dynamics of various PM-16QAM super-channel structures (240Gb/s, 480Gb/s and 1.2Tb/s). We confirmed that homogeneous spectrum allocation may be employed in flex-networks, with negligible performance penalty, allowing minimal fragmentation scenarios. In particular, we showed that for high dispersion fibers, homogeneous and heterogeneous spectrum allocation enables similar performance, within ~0.5dB, and the absolute penalties are found to be less than ~1dB. On the other hand, for low dispersion fibers, heterogeneous spectrum allocation employing 120Gb/s PM-QPSK enables the optimal performance, whereas homogeneous spectrum allocation is only 0.5dB away from the optimal solution, with absolute performance penalties limited to less than ~1.5dB

From our results it can be concluded that in vast majority of network scenarios, additional band-gap between super-channels and co-propagating traffic is not necessarily required (relative penalties below ~1dB), and occurrence of stranded bandwidth in flex-networks can be avoided. Moreover, independent of the traffic patter, i.e. growth only or fully dynamic, both homogenous and heterogeneous may be employed.

Acknowledgment

This work was supported by the German Federal Ministry of Education and Research (BMBF) under grant number 01BP12300A, EUREKA-Project SASER.

#194912 - $15.00 USD Received 30 Jul 2013; revised 11 Oct 2013; accepted 15 Nov 2013; published 19 Dec 2013